ELSEVIER

Chemical Engineering Journal 84 (2001) 335–342

Chemical Engineering Journal

www.elsevier.com/locate/cej

Radiation effects on free convection flow past a semi-infinite vertical plate with mass transfer

A.J. Chamkha [a,*], H.S. Takhar [b], V.M. Soundalgekar [c]

[a] *Department of Mechanical and Industrial Engineering, Kuwait University, Safat 13060, Kuwait*
[b] *School of Engineering, Manchester University, Manchester M13 9PL, UK*
[c] *31A-12, Brindavan Society, Thane 400601, India*

Received 22 February 2000; received in revised form 13 November 2000; accepted 20 November 2000

Abstract

Laminar free convection flow of air past a semi-infinite vertical plate in the presence of chemical species concentration and thermal radiation effects is studied. This type of problem finds application in many technological and engineering fields such as rocket propulsion systems, spacecraft re-entry aerothermodynamics, cosmical flight aerodynamics, plasma physics, glass production and furnace engineering. The governing boundary-layer equations for this problem are reduced to a non-similar form and are solved numerically by an implicit finite-difference technique. Representative velocity, temperature and concentration profiles are shown graphically and the numerical values of the wall slopes of the velocity, temperature and concentration profiles (which are related to the dimensionless skin-friction coefficient, wall heat transfer and the Sherwood number, respectively) are also shown graphically. The effects of the radiation parameter, buoyancy ratio, Schmidt number and the dimensionless distance from the leading edge of the plate on the numerical solutions are presented and discussed.

Keywords: Laminar free convection flow; Cosmic flight aerodynamics; Sherwood number

1. Introduction

Pohlhausen [1] first studied the free convection flow past a semi-infinite vertical plate by the momentum integral method because free convection flows have wide applications in industry. But the similarity solution to free convection flow past a semi-infinite vertical plate was first presented by Ostrach [2] who solved the non-linear coupled ordinary differential equations numerically on a computer. The fluid considered was air. Later on, many papers were published on this topic under different physical conditions and these are referred in a book by Gebhart et al. [3]. The fluid considered in all these studies was either pure air or water. However, in nature, pure air or water is not easily available and hence, the results already presented in [1,2] are not general in nature. As a simple example, atmospheric flows, at all scales are driven appreciably by both temperature and H_2O concentrated differences. In water, dissolved materials, suspended particulate matter are always present and hence, the density is affected by both temperature and concentration. These are described in the literature as mass transfer effects. The effects of foreign masses, also known as diffusing species concentration, were studied under different conditions by Somers [4], Mathers et al. [5], Wilcox [6], Gill et al. [7], Lowell and Admas [8], Adams and Lowell [9], Cardner and Hellums [10], etc. either by an integral method or an asymptotic analysis. It was also assumed that the species concentration level present in air or water was at low level and hence, other effects like Soret and Dufour effects were negligible. But the first systematic study of mass transfer effects on free convection flow past a semi-infinite vertical plate was presented by Gebhart and Pera [11], who presented a similarity solution to this problem and introduced a parameter N which is a measure of the relative importance of chemical and thermal diffusion in causing the density difference that drives the flow. The parameter N is positive when both effects combine to drive the flow and it is negative when these effects are opposed. Gebhart [12] also derived the boundary-layer equations governing free convection flows with mass transfer on the assumption of low level of species concentration present in the fluid.

In all these investigation, radiation effects are neglected. For some industrial applications such as glass production and furnace design and in space technology applications, such as cosmical flight aerodynamics rocket,

* Corresponding author. Tel.: +965-484-9413; fax: +965-484-7131.

1385-8947/01/$ – see front matter
PII: S1385-8947(00)00378-8

Nomenclature

c_p	specific heat at constant pressure
C	species concentration
D	species diffusivity
$e_{b\lambda}$	Plank's function
F	dimensionless stream function ($F = \psi/4\nu C_1 x^{3/4}$)
F_L	radiation parameter ($F_L = 4IL^2/\rho c_p \nu\sqrt{C_1}$)
g	gravitational acceleration
k	thermal conductivity
K_λ	absorption coefficient
L	characteristic length
N	buoyancy ratio parameter ($N = \beta^*(c_w - c_\infty)/\beta(T_w - T_\infty)$)
Pr	Prandtl number ($Pr = \rho\nu c_p/k$)
q	wall rate of heat transfer defined by Eq. (16)
q_r	thermal radiation flux defined by Eq. (1)
Sc	Schmidt number ($Sc = \nu/D$)
SHQ	wall rate of mass transfer defined by Eq. (18)
T	temperature
u	x-component of velocity
v	y-component of velocity
x, y	Cartersian coordinate system

Greek Symbols

β	thermal expansion coefficient
β^*	species expansion coefficient
η	transformed normal coordinate
μ	dynamic viscosity
ν	kinematic viscosity
ϕ	dimensionless species concentration ($\phi = (c - c_\infty)/(c_w - c_\infty)$)
ρ	density
ψ	stream function
θ	dimensionless temperature ($\theta = (T - T_\infty)/(T_w - T_\infty)$)
τ	skin-friction defined by Eq. (15)
ξ	dimensionless distance along the plate ($\xi = (x/L)^{1/2}$)

Subscripts

w	wall
∞	free stream

propulsion systems, plasma physics and spacecraft re-entry aerothermodynamics which operate at higher temperatures, radiation effects can be significant. When radiation is taken into account, the governing equations become quite complicated and hence, many difficulties arise while solving such equations. However, Greif et al. [13] have shown that in the optically thin limit, the physical situation can be simplified and then they derived an exact solution to fully-developed vertical channel flow for a radiative fluid. Cogley et al. [14], had shown that for an optically thin limit, the fluid does not absorb its own emitted radiation or there is no self-absorption, but the fluid does absorb radiation emitted by the boundaries. It was shown by Cogley et al. [14] that in the optically thin limit for a gray-gas near equilibrium, the following relation holds

$$\frac{dq_r}{dy} = 4(T - T_w)I \tag{1}$$

where

$$I = \int_0^\infty K_{\lambda w}\left(\frac{\partial e_{b\lambda}}{\partial T}\right)_w d\lambda$$

All the physical quantities are defined in the nomenclature. Based on this assumption, we now propose to study the free convection flow of a radiative gas, in the optically thin limit, in the presence of foreign mass at a low level. This enables us to neglect Soret and Dufour effects.

2. Mathematical analysis

Consider the flow of a gray-gas near equilibrium in the optically thin limit, past a semi-infinite vertical plate. The x-axis is taken along the vertical plate in the upward direction and the y-axis is taken normal to the plate. The flow is driven by buoyancy effects, which are generated by gradients in temperature and in the concentration field of a dissolved species. If the characteristic parameter of free convection, that is the Grashof number, is increased to infinity, the flow along a vertical heated plate based on the solution of the Navier–Stokes equations becomes identical to the solution of the boundary-layer equations. Assuming negligible viscous dissipative heat, the boundary-layer form of the governing equations along with the Boussinesq approximation for steady, laminar, free convective flow of a radiative gray-gas is given by

$$\frac{\partial u}{\partial x} + \frac{\partial v}{\partial y} = 0 \tag{2}$$

$$\rho\left(u\frac{\partial u}{\partial x} + v\frac{\partial u}{\partial y}\right) = \mu\frac{\partial^2 u}{\partial y^2} + \rho g\beta(T - T_\infty) + \rho g\beta^*(c - c_\infty) \tag{3}$$

$$\rho c_p\left(u\frac{\partial T}{\partial x} + v\frac{\partial T}{\partial y}\right) = k\frac{\partial^2 T}{\partial y^2} - \frac{\partial q_r}{\partial y} \tag{4}$$

$$u\frac{\partial c}{\partial x} + v\frac{\partial c}{\partial y} = D\frac{\partial^2 c}{\partial y^2} \tag{5}$$

All the physical variables are defined in the nomenclature. The boundary conditions are now given by

$$u = 0, \quad v = 0, \quad T = T_w, \quad c = c_w \text{ at } y = 0$$
$$u = 0, \quad T \to T_\infty, \quad c \to c_\infty \text{ as } y \to \infty \tag{6}$$

The first two conditions indicate that the fluid does not slip at the boundary and that the plate is impermeable to mass transfer. The second two conditions suggest that both the fluid temperature and the species concentration are constant at the plate surface. The last three conditions imply that the ambient fluid far away from the plate surface is stagnant and at uniform temperature and species concentration. The assumptions of constant wall and ambient concentrations are somewhat idealistic. Nevertheless, in some controlled experiments, very close situations can be achieved.

Now, due to the presence of a radiation term, the similarity solution is not possible. So, we seek a non-similar solution. We define the following variables

$$\eta = C_1 y x^{-1/4}, \quad C_1 = \left(\frac{g\beta\Delta T}{4\nu^2}\right)^{1/4},$$
$$\Delta T = T_w - T_\infty = \text{constant}$$

$$\theta = \frac{T - T_\infty}{T_w - T_\infty},$$
$$C = \frac{g\beta L^3 \Delta T}{\nu^2} \text{ and hence } C_1 = \left(\frac{C}{4}\right)^{1/4} L^{-3/4}$$

$$Pr = \rho\nu\frac{c_p}{k}, \quad Sc = \frac{\nu}{D}, \quad \xi = \left(\frac{x}{L}\right)^{1/2}$$

$$\phi = \frac{c - c_\infty}{c_w - c_\infty}, \quad \psi = 4\nu C_1 x^{3/4} F(\xi, \eta) \tag{7}$$

Then we have

$$\frac{\partial}{\partial y} = \frac{\partial}{\partial \eta}\frac{\partial \eta}{\partial y} = C_1 x^{-1/4}\frac{\partial}{\partial \eta}$$

$$\frac{\partial^2}{\partial y^2} = \frac{\partial}{\partial \eta}\left(\frac{\partial}{\partial y}\right)\frac{\partial \eta}{\partial y} = C_1^2 x^{-1/2}\frac{\partial^2}{\partial \eta^2}$$

$$\frac{\partial}{\partial x} = \frac{\partial}{\partial x} + \frac{\partial}{\partial \eta}\frac{\partial \eta}{\partial x} = \frac{\partial}{\partial x} - \left(\frac{1}{4}\right)x^{-5/4} C_1 y \frac{\partial}{\partial \eta}$$
$$= \frac{\partial}{\partial x} - \frac{1}{4}\frac{\eta}{x}\frac{\partial}{\partial \eta}$$

$$\frac{\partial \xi}{\partial x} = \frac{1}{2}\frac{\xi}{x}$$

$$u = \frac{\partial \psi}{\partial y} = -C_1 x^{-1/4}\frac{\partial}{\partial \eta}(4\nu C_1 x^{3/4} F(\xi, \eta))$$
$$= 4\nu C_1^2 x^{1/2} F'(\xi, \eta) \tag{8}$$

$$v = -\frac{\partial \psi}{\partial x} = -\left(\frac{\partial}{\partial x} - \frac{1}{4}\frac{\eta}{x}\frac{\partial}{\partial \eta}\right)(4\nu C_1 x^{3/4} F(\xi, \eta))$$
$$= 4\nu C_1\left(\frac{3}{4}x^{-1/4} F(\xi, \eta) + x^{3/4}\frac{\partial F}{\partial \xi}\frac{1}{2}\frac{\xi}{x} - \frac{1}{4}\frac{\eta}{x}x^{3/4} F'\right)$$
$$= \nu C_1 x^{-1/4}\left(3F + 2\xi\frac{\partial F}{\partial \xi} - \eta F'\right) \tag{9}$$

Substituting the above relations in Eq. (3) and simplifying, we have

$$F''' + 3FF'' - 2(F')^2 + 2\xi\left(F''\frac{\partial F}{\partial \xi} - F'\frac{\partial^2 F}{\partial \xi \partial \eta}\right) + \theta + N\phi = 0 \tag{10}$$

where a prime denotes partial differentiation with respect to η and $N = \beta^*(c_w - c_\infty)/\beta(T_w - T_\infty)$ is the buoyancy ratio parameter.

Eq. (4) with above relations and (1), (8) and (9) now reduce to

$$\frac{1}{Pr}\theta'' + 3F\theta' + 2\xi\left(\theta'\frac{\partial F}{\partial \xi} - F'\frac{\partial \theta}{\partial \xi}\right) - 2\xi F_L \theta = 0 \tag{11}$$

Here F_L is the radiation parameter and is defined as

$$F_L = \frac{4IL^2}{\rho c_p \nu\sqrt{C_1}}$$

and Eq. (5) now reduces to

$$\frac{1}{Sc}\phi'' + 3F\phi' + 2\xi\left(\phi'\frac{\partial F}{\partial \xi} - F'\frac{\partial \phi}{\partial \xi}\right) = 0 \tag{12}$$

Here Pr and Sc are respectively, the Prandtl and Schmidt numbers. The advantage of Eq. (10) through (12) is that they produce their own initial profiles at $\xi = 0$ by the solution of the self-similar ordinary differential equations which result there. In addition, less numerical efforts are required to solve Eq. (10) through (12) than to solve Eq. (2) through (5).

The corresponding dimensionless boundary conditions are

$$\begin{aligned} F(0) = F'(0) = 0, &\qquad F'(\infty) = 0 \\ \theta(0) = 1, &\qquad \phi(0) = 1 \\ \theta(\infty) = 0, &\qquad \phi(\infty) = 0 \end{aligned} \tag{13}$$

In order to understand the physical aspect of the problem, we have solved Eqs. (10)–(12) under boundary conditions (13) numerically by an implicit, iterative, tridigonal finite-difference method similar to that discussed by Blottner [14]. The method is described as follows.

All first-order derivatives with respect to ξ are replaced by two-point backward difference formulae of the form

$$\frac{\partial A}{\partial \xi} = \frac{A_{m,n} - A_{m-1,n}}{\Delta \xi} \tag{14}$$

where A is any dependent variable and m and n are node locations along the ξ and η directions, respectively. The third-order differential Eq. (10) is converted into a second-order one by substituting $V = F'$. Then all second-order equations for V, θ and ϕ are discretized using three-point central difference quotients while the first-order differential equation governing F is discretized by the trapezoidal rule. At each line of constant ξ, a set of algebraic equations results. With the non-linear terms evaluated at the previous iteration, the algebraic equations are solved with iteration by the well-known Thomas algorithm (see Blottner

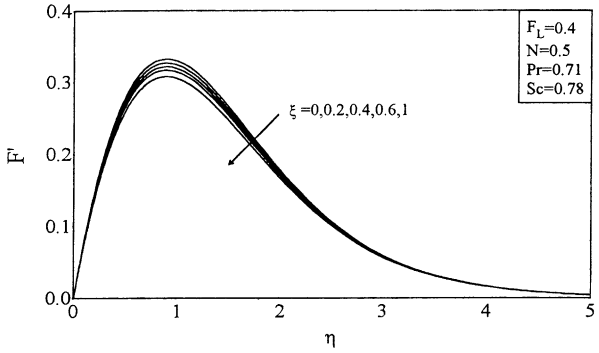

Fig. 1. Development of velocity profiles with ξ.

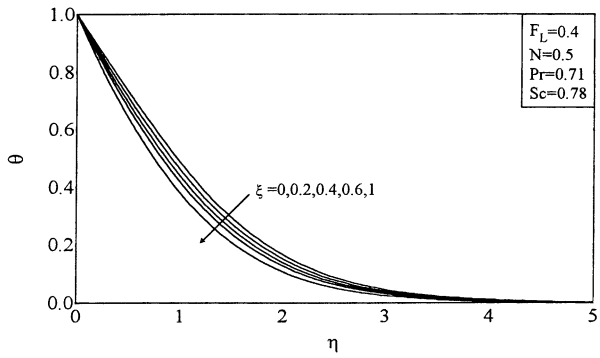

Fig. 2. Development of temperature profiles with ξ.

[15]). The same process is repeated for the next ξ value and the problem is solved line by line until $\xi = 1$ is reached. A convergence criterion based on the relative difference between the current and the previous iterations is employed. When this difference reaches 10^{-5}, the solution is assumed converged and the iteration process is terminated. A representative set of numerical results is shown graphically in Figs. 1–21, to illustrate the influence of various parameters on the velocity, temperature and concentration profiles. The flow of air ($Pr = 0.71$) is assumed and then the corresponding values of the Schmidt number are as given by Gebhart and Pera [11] Table 1.

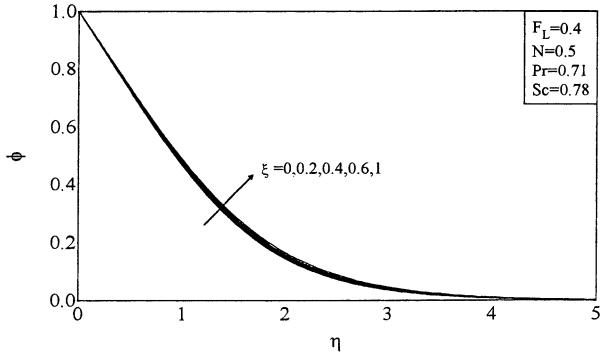

Fig. 3. Development of concentration profiles with ξ.

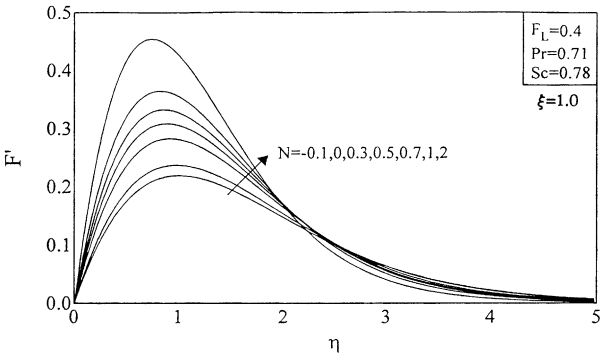

Fig. 4. Effects of N on velocity profiles.

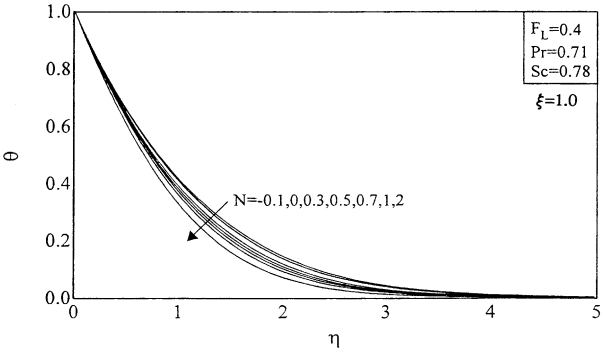

Fig. 5. Effects of N on temperature profiles.

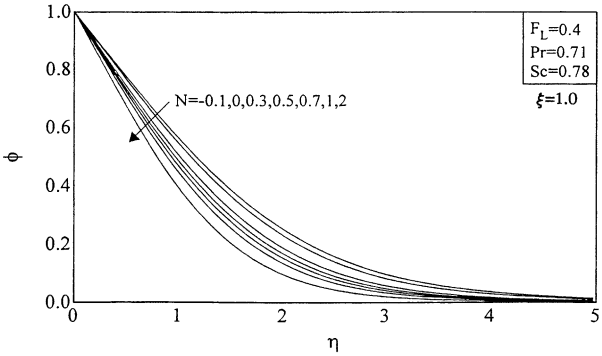

Fig. 6. Effects of N on concentration profiles.

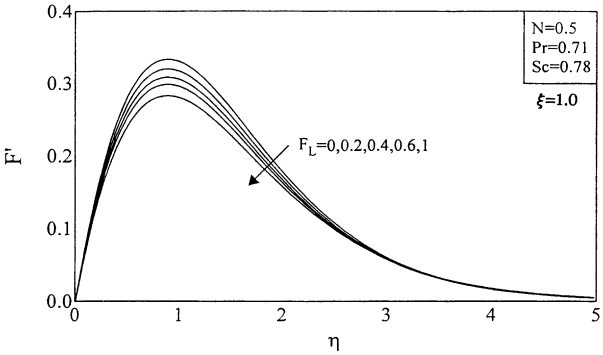

Fig. 7. Effects of F_L on velocity profiles.

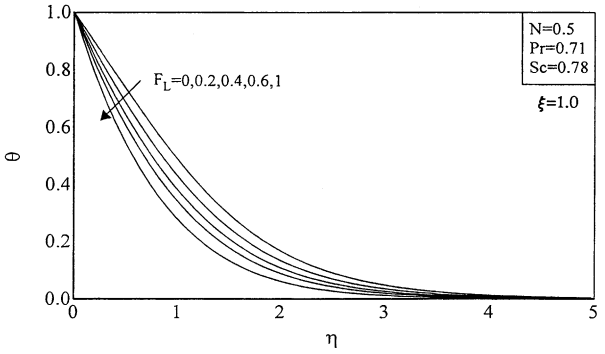

Fig. 8. Effects of F_L on temperature profiles.

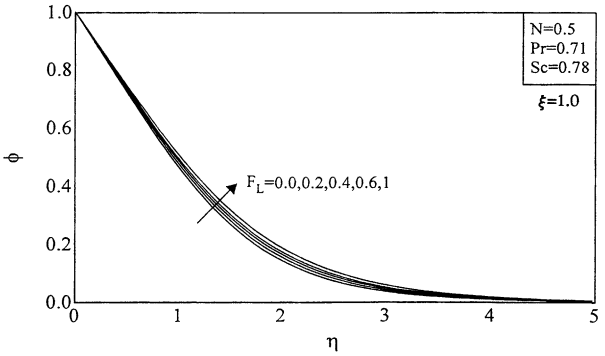

Fig. 9. Effects of F_L on concentration profiles.

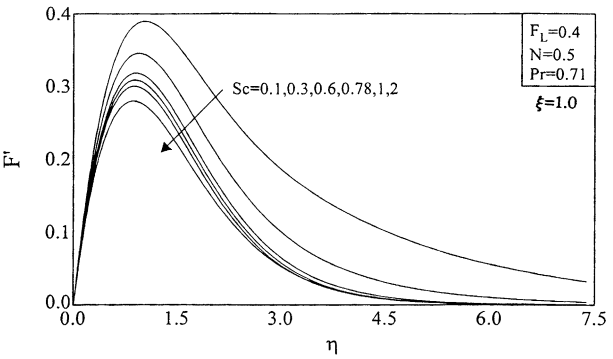

Fig. 10. Effects of *Sc* on velocity profiles.

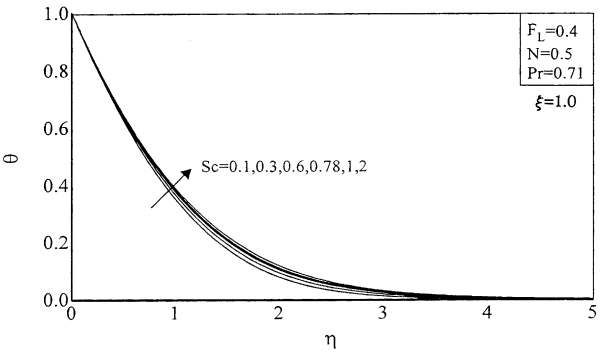

Fig. 11. Effects of *Sc* on temperature profiles.

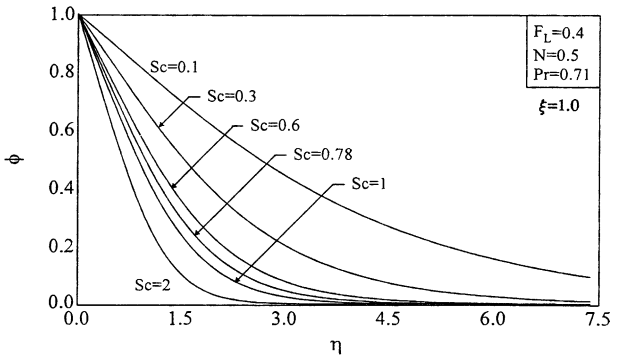

Fig. 12. Effects of *Sc* on concentration profiles.

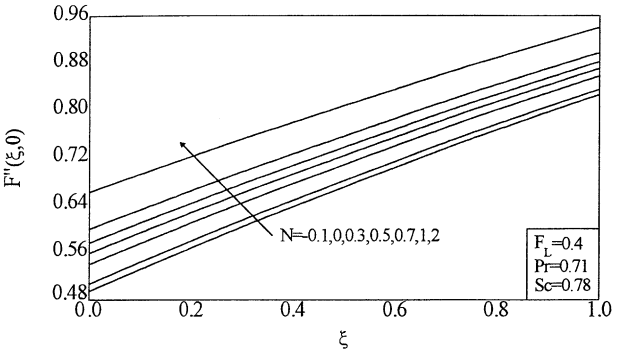

Fig. 13. Effects of *N* on skin-friction coefficient.

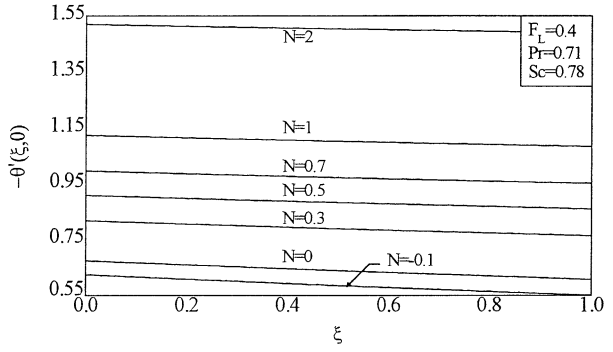

Fig. 14. Effects of *N* on wall heat transfer.

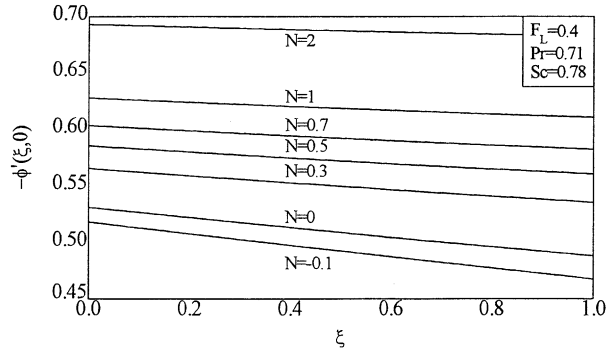

Fig. 15. Effects of *N* on Sherwood number.

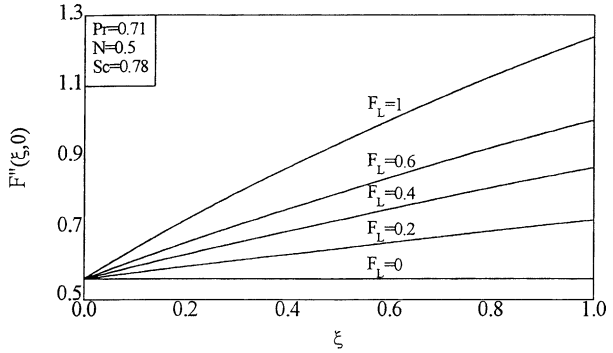

Fig. 16. Effects of F_L on skin-friction coefficient.

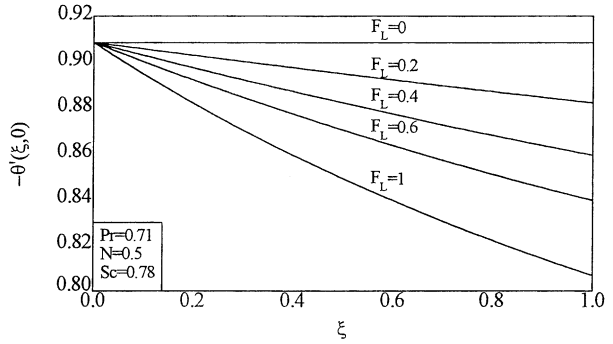

Fig. 17. Effects of F_L on wall heat transfer.

So in air, the diffusing chemical species of most common interest have Schmidt numbers in the range of 0.1–2. The buoyancy ratio parameter N also plays an important role. The chemical and thermal diffusion causes the density difference that drives the flow. The negative values of N indicate the effect of opposing buoyancy mechanism whereas the positive values of N indicate the effect of aiding buoyancy mechanism. Also, the quantity ξ represents the distance of a point from the leading edge. So we consider here the effects of these parameters Sc, N, ξ and F_L on the flow of air, $Pr = 0.71$.

The effect of ξ on the velocity, temperature and concentration profiles is shown in Figs. 1–3. We observe from these

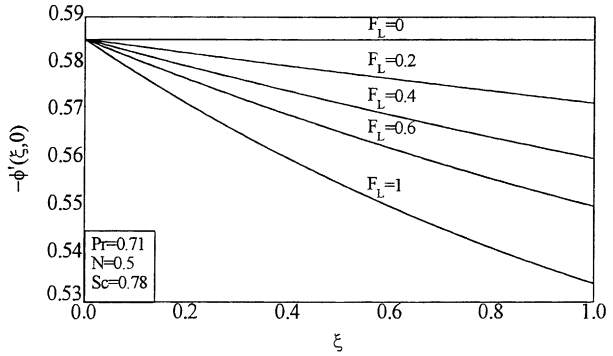

Fig. 18. Effects of F_L on Sherwood number.

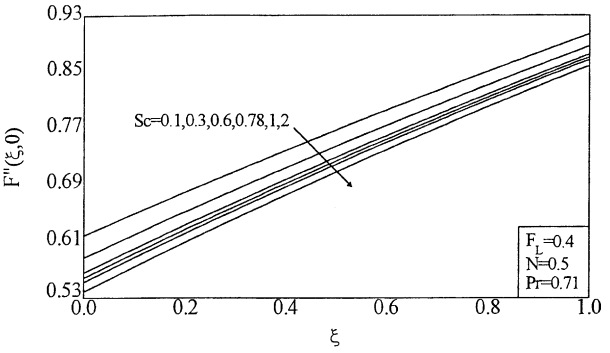

Fig. 19. Effects of Sc on skin-friction coefficient.

figures that as the distance from the leading edge increases, both the velocity and temperature decrease whereas the concentration increases when F_L, N, and Sc are constant. The effect of the buoyancy ratio parameter N on the velocity, temperature and concentration profiles is shown at $\xi = 1$, $F_L = 0.4$, $Sc = 0.78$ in Figs. 4–6. We observe from these figures that when there is an opposing buoyancy force, the velocity is less but the temperature and concentration are more as compared to that in the presence of an aiding buoyancy force. The velocity is also found to increase as the aiding buoyancy force increases. But both the temperature and concentration decrease as the aiding buoyancy force increases. The effect of the radiation parameter F_L on the velocity, temperature and the concentration profiles is shown in Figs. 7–9, at $\xi = 1$, $N = 0.5$, $Pr = 0.71$ and $Sc = 0.78$. We observe from these figures that an increase in the radiation parameter F_L leads to a decrease in the velocity and temperature but an increase in the concentration profile. The effect of foreign mass on the velocity, temperature and concentration profiles is shown in Figs. 10–12 and we observe that an increase in the Schmidt number Sc leads to a decrease in the velocity and concentration but an increase in the temperature in the presence of an aiding buoyancy force.

Knowing the velocity, temperature and concentration fields, it is important to study the effects of these parameters on the skin-friction, rate of heat transfer and the rate of mass transfer at the plate.

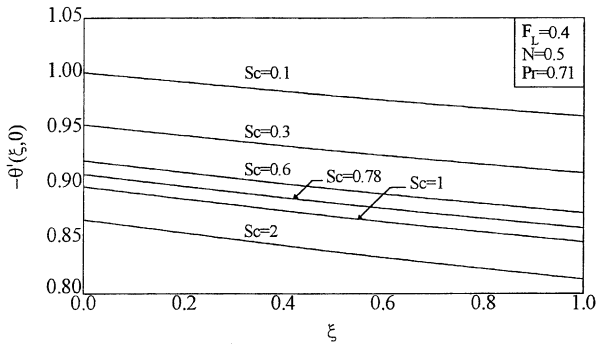

Fig. 20. Effects of Sc on wall heat transfer.

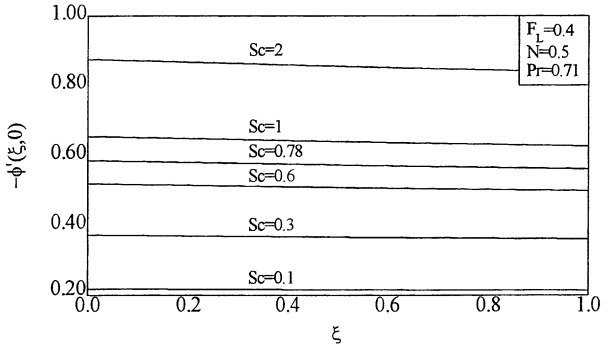

Fig. 21. Effects of *Sc* on Sherwood number.

The dimensional skin-friction is given by

$$\tau = -\mu \left(\frac{\partial u}{\partial y}\right)_{y=0} \tag{15}$$

and in view of (7) and (8), it reduces to

$$\tau = -4\mu\nu C_1^3 x^{1/2} F''(\xi, 0)$$

The rate of heat transfer in dimensional form is given by

$$q = -k \left.\frac{\partial T}{\partial y}\right|_{y=0} + q_r|_{y=0} \tag{16}$$

and in view of (7), (16) reduces to

$$q = -k\Delta T C_1 x^{-1/4} \left.\frac{\partial \theta}{\partial \eta}\right|_{\eta=0} + 4I\Delta T \int_o^\infty \theta \, dy$$

$$= k\Delta T C_1 x^{-1/4} \theta'(\xi, 0) + \frac{4I\Delta T x^{1/4}}{C_1} \int_o^\infty \theta \, d\eta \tag{17}$$

The rate of mass transfer is given by

$$\mathrm{SHQ} = -D \left.\frac{\partial c}{\partial y}\right|_{y=0} \tag{18}$$

$$\mathrm{SHQ} = D\Delta c C_1 x^{-1/4} \left.\frac{\partial \phi}{\partial \eta}\right|_{\eta=0}$$

$$= -D\Delta c C_1 x^{-1/4} \phi'(\xi, 0) \tag{19}$$

Table 1
Values of the Schmidt number of various species or low concentration in air at approximately 25°C and 1 atm

Species	*Sc*
Ammonia	0.78
Carbon dioxide (CO_2)	0.94
Hydrogen	0.22
Oxygen (O_2)	0.75
Water vapor	0.60
Benzene	1.76
Ether	1.66
Methanol	0.97
Ethyl alcohol	1.30
Ethyl benzene	2.01

where $\Delta c = c_w - c_\infty$ is the difference between the wall and free stream concentrations.

We have computed numerical values of $\{-F''(\xi, 0)\}$, $\{-\theta'(\xi, 0)\}$ and $\{-\phi'(\xi, 0)\}$ and the effects of the different parameters F_L, N and Sc on these quantities are shown in Figs. 13–21.

The effects of the buoyancy force parameter N on $\{-F''(\xi, 0)\}$, $\{-\theta'(\xi, 0)\}$ and $\{-\phi'(\xi, 0)\}$ are shown in Figs. 13–15, respectively. We observe from Fig. 13 that the value of $\{-F''(\xi, 0)\}$ is more in the presence of aiding buoyancy parameter ($+N$) as compared to opposing buoyancy parameter ($-N$) and it increases with an increase in ($+N$) and ξ. The effect of ($+N$) is the same for the rate of heat transfer and the Sherwood number, but the rate of heat transfer $\{-\theta'(\xi, 0)\}$ and the Sherwood number decrease with increasing values of ξ. The effect of the radiation parameter F_L on the skin-friction, rate of heat transfer and the Sherwood number for $N = 0.5$ and $Sc = 0.78$ is shown in Figs. 16–18, respectively. We observe from these figures that $\{-F''(\xi, 0)\}$ increases and $\{-\theta'(\xi, 0)\}$ and $\{-\phi'(\xi, 0)\}$ decreases in F_L. However, the skin-friction coefficient increases with increasing values of ξ and $\{-\theta'(\xi, 0)\}$ and $\{-\phi'(\xi, 0)\}$ decrease with increasing values of ξ. That is, they decrease as the distance along the plate increases. The effect of the Schmidt number Sc on $\{-F''(\xi, 0)\}$, $\{-\theta'(\xi, 0)\}$ and $\{-\phi'(\xi, 0)\}$ is shown in Figs. 19–21, respectively. We conclude from these figures that the values of $\{-F''(\xi, 0)\}$, $\{-\theta'(\xi, 0)\}$ and $\{-\phi'(\xi, 0)\}$ decrease with an increase in the value of the Schmidt number Sc but $\{-F''(\xi, 0)\}$ increases very rapidly as the distance along the plate increases. However, the values of $\{-\theta'(\xi, 0)\}$ and $\{-\phi'(\xi, 0)\}$ decrease along the plate as the value of ξ increases.

3. Conclusions

This paper considered steady, laminar free convection flow of an optically-thin gray-gas with dissolved chemical species along a semi-infinite vertical plate in the presence of thermal radiation effects. The governing equations were non-dimensionalized and transformed into a non-similar form. The transformed equations were solved numerically using an implicit finite-difference method. A representative set of the obtained results for the velocity, temperature, and concentration profiles as well as the skin-friction coefficient, wall heat transfer and the Sherwood number was reported graphically for various parametric conditions. The following points were concluded.

1. Both the velocity and temperature decreased as the distance from the plate's leading edge was increased.
2. In the presence of an opposing buoyancy force, the velocity was less but both the temperature and concentration were more. In the presence of an aiding buoyancy force, however, an increase in the buoyancy ratio led to an increase in the velocity and decreases in both the temperature and concentration.

3. An increase in the radiation parameter led to decreases in both the velocity and temperature but an increase in the concentration.
4. An increase in the values of the Schmidt number resulted in decreases in both the velocity and concentration but an increase in the temperature of air in the presence of an aiding buoyancy force.
5. The dimensionless skin-friction coefficient increased with increasing values of the buoyancy ratio (for both aiding and opposing flows), radiation parameter, Schmidt number, and the distance from the plate's leading edge. The negative slope of the temperature profile which is related to the wall heat transfer increased with increases in the values of the buoyancy ratio but it decreased with increasing values of the radiation parameter or the Schmidt number. The dimensionless rate of mass transfer or the Sherwood number increased with increasing values of the buoyancy ratio or the Schmidt number but it decreased with increasing values of the radiation parameter.

It is hoped that the present results will be used as a vehicle for comparison with more complicated problems dealing with heat and mass transfer in the presence of radiation.

References

[1] H. Pohlhausen, Der Warmeaustrausch zwischen festen Korpern und Flussigkeiten mit Kleiner Reibung under Kleiner Warmeleitung, ZAMM 1 (1921) 115–121.
[2] S. Ostrach, An analysis of laminar free convection flow and heat transfer along a flat plate parallel to the direction of the generating body force, NACA Report 1111, 1953.
[3] B. Gebhart, Y. Jaluria, R.L. Mahajan, B, Sammakia, Buoyancy Induced Flows and Transport, Hemisphere, Washington, DC, 1988, pp. 1–100.
[4] E.V. Somers, Theoretical considerations of combined thermal and mass transfer from a vertical flat plate, J. Appl. Mech. 23 (1956) 295–301.
[5] W.G. Mathers, A.J. Madden, E.L. Piret, Simultaneous heat and mass transfer in free convection, Ind. Eng. Chem. 49 (1957) 961–968.
[6] W.R. Wilcox, Simultaneous heat and mass transfer in free convection, Chem. Eng. Sci. 13 (1961) 113–119.
[7] W.N. Gill, E. Del Casal, D.W. Zeh, Binary diffusion and heat transfer in laminar free convection boundary layers on a vertical plate, Int. J. Heat Mass Transfer 8 (1965) 1131–1151.
[8] R.L. Lowell, J.A. Adams, Similarity analysis for multicomponent free convection, AIAA J. 5 (1967) 1360–1364.
[9] J.A. Adams, R.L. Lowell, Free convection organic sublimation on a vertical semi-infinite plate, Int. J. Heat Mass Transfer 11 (1968) 1215–1224.
[10] D.V. Cardner, J.D. Hellums, Simultaneous heat and mass transfer in laminar free convection with a moving interface, I/EC Fundam. 6 (1967) 376–380.
[11] B. Gebhart, L. Pera, The nature of vertical natural convection flows resulting from the combined buoyancy effects of thermal and mass diffusion, Int. J. Heat Mass Transfer 14 (1971) 2025–2050.
[12] B. Gebhart, Heat Transfer, 2nd Edition, McGraw-Hill, New York, 1971.
[13] R. Grief, I.S. Habib, L.C. Lin, Laminar convection of a radiating gas in a vertical channel, J. Fluid Mech. 45 (1971) 513–520.
[14] A.C. Cogley, W.G. Vincenti, S.E. Gill, Differential approximation for radiative transfer in a non-gray-gas near equilibrium, AIAA J. 6 (1968) 551–553.
[15] F.G. Blottner, Finite-difference methods of solution of the boundary-layer equations, AIAA J. 8 (1970) 193–205.